# Ruthenium complexes containing mPTA and the thiopurines bis(8-thiotheophylline)-$(CH_2)_n$ and mPTA (n= 1-3; mPTA = N-methyl-1,3,5-triaza-7-phosphaadamantane).

Lazhar Hajji[a], Cristobal Saraiba Bello[a], Franco Scalambra[a], Gaspar Segovia-Torrente[a], Antonio Romerosa*[a], A. Canella[b].

[a]*Área de Química Inorgánica-CIESOL, Facultad de Ciencias Experimentales, Universidad de Almería, 04071 Almería – Spain.*

[b]*Dipartimento di Biochimica e Biologia Moleculare dell'Università d Ferrara, via L. Borsari 46, 44100 Ferrara, Italy.*

*E-mail address: romerosa@ual.es*

## ABSTRACT

Thiopurines bis(S-8-thiotheophylline)methane ($MBTTH_2$), 1,2-bis(S-8-thiotheophylline)ethane ($EBTTH_2$) and 1,3-bis(S-8-thiotheophylline)propane ($PBTTH_2$) were reacted with $[RuClCp(mPTA)_2](CF_3SO_3)_2$ in water to afford the bi-ruthenium complexes $[\{RuCp(mPTA)_2\}_2$-μ-(L-κ*N7,N´7*)$](CF_3SO_3)_4$ (**1**: L = MBTT; **2**: L = EBTT; **3**: L = PBTT), which have been characterized by elemental analysis, IR and NMR multinuclear ($^1H$, $^{13}C\{^1H\}$, $^{31}P\{^1H\}$ and $^{19}F\{^1H\}$) spectroscopy. Diffusion experiments for **1** were carried out. Proposed structures for the three complexes were also supported by theoretical calculations. Their cyclic voltammetry showed that all these complexes are characterized by two one-electron irreversible oxidative responses ($Ru^{II}$–$Ru^{II}$/$Ru^{III}$–$Ru^{II}$; $Ru^{III}$–$Ru^{II}$/$Ru^{III}$–$Ru^{III}$). Complexes showed pour antiplorifelative activity against *cis*platin-sensitive T2 human cell line and the *cis*platin-resistant SKOV3 cell line.

Keywords: Ruthenium complexes; mPTA; Bis-thiotheophylline; Water-soluble complexes; Electrochemistry.

## 1. Introduction

The *cis*platin is one of the most widely used drugs for treatment of cancer [1,2]. Despite of its wide applicability this drug displays high toxicity, producing severe side effects. Another important problem is the lack of general activity [3]. To overcome these problems many attempts have been done, being one of the most useful strategy to develop alternatives to platinum based drugs [4]. The ruthenium complexes have shown to be one of the most valuable candidates to substitute the platinum compounds. Ruthenium complexes use to be characterized by variable oxidation states, low toxicity, selectivity for cancer cells and ability to mimic iron in binding to biomolecules [5]. Two of the most promising ruthenium complexes as new anticancer drugs are the KP1019 and NAMI-A, which are in the last clinical evaluation stages [6]. Notably, these complexes exhibit a comparable to *cis*platin antitumor properties but with lest toxicity and related side effects [3-5]. One of the valuable properties of the complexes to be a drug is their capacity of dissolving in water as the natural life is constituted mainly by this solvent. Our research team aimed the synthesis of new anticancer-active platinum and ruthenium complexes soluble in water, some of them with better activity than *cis*platin [7]. Some of these complexes contain water-soluble phosphines such as PTA and its derivatives mPTA and dmPTA (PTA = 1,3,5-triaza-7-phosphaadamantane; mPTA = N-methyl-1,3,5-triaza-7-phosphaadamantane; dmPTA = N,N′-dimethyl-1,3,5-triaza-7-phosphaadamantane) [8]. To obtain additional information on how the ruthenium complexes containing PTA and mPTA interact with purines their reactivity with thio- and bis-thio-theophyllines were evaluated. The thio-derivatives show interesting properties useful to obtain initial information on how the metal complexes could acts on the purines. They have only a limited number of coordination positions in contrast with DNA-purines as well as more solubility in organic solvents and groups active in $^{1}H$ and $^{13}C$ NMR. Bis-thiopurines are particularly interesting as they

bear two purines depending on the length of the spacing group. This disposition of the purines could mimic the DNA, providing easily interesting information that could be useful for understand how metal complexes could interact with DNA. In previous papers we have published the reactivity of water-soluble ruthenium(II) mononuclear complexes [RuClCp(PTA)(L)] with bis-thiotheophyllines (Figure 1) that provided binuclear complexes [{RuCp(PTA)(L)}$_2$-μ-(Y-κ*S,S′*)] (Y = MBTT$^{2-}$, EBTT$^{2-}$, PBTT$^{2-}$; L = PTA, PPh$_3$) [9]. The evaluation of the anticancer activity of these complexes against *cis*platin-sensitive T2 and *cis*platin-resistant SKOV3 cell lines showed that these complexes do not display significant antiproliferative activity. Complexes [{RuCp(PPh$_3$)(mPTA)}$_2$-μ-(Y-κ*S,S′*)] showed that the combination of bispurines with ruthenium with mPTA, soluble in water, and PPh$_3$, soluble in organic solvents, are non-reactive against DNA. Their low solubility in the standard dmso/water mixture avoided the evaluation of their antiproliferative activity against living cells [10]. Nevertheless, these complexes showed that their oxidation potentials are related with the purine linking group size. To determine if this behavior is reproducible and independent of the phosphine bonded to the metal and if a water soluble parent complexes display antiproliferative activity, three new water-soluble neutral binuclear ruthenium complexes [{RuCp(mPTA)$_2$}$_2$-μ-(Y-κ*S7,S′7*)](CF$_3$SO$_3$)$_4$ were synthesized and their redox properties studied, which are similar to those previously studied but in which the metal is bonded to two mPTA instead to one mPTA and one PPh$_3$.

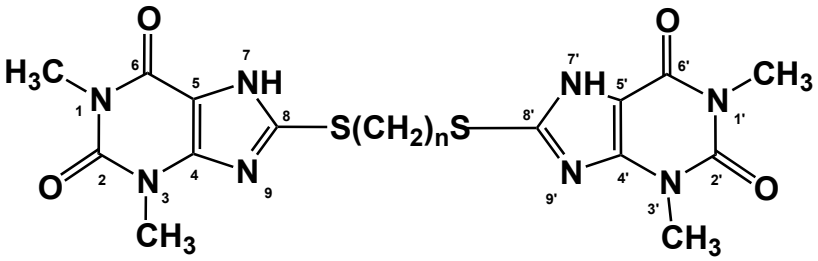


**Y: n = 1 (MBTTH$_2$); n = 2 (EBTTH$_2$); n = 3 (PBTTH$_2$)**

Figure 1. Chemical structure of 8-bis-thiopurines

## 2. Experimental

### 2.1. General procedures

All reactions and manipulations were routinely performed under a dry nitrogen atmosphere by using standard Schlenk-tube techniques. All chemicals were reagent grade and were used as received by commercial suppliers unless otherwise stated. The solvents were all degassed and distilled according to standard procedures [11]. The compounds mPTA, $[RuClCp(mPTA)_2](CF_3SO_3)_2$ and bis(8-thiotheophylline) alkane derivatives $MBTTH_2$, $EBTTH_2$ and $PBTTH_2$ were prepared following the procedure described in literature [12]. Solvents for NMR measurements (Cortec-Euriso-top) were dried over molecular sieves (0.4 nm). $^{1}H$, $^{31}P\{^{1}H\}$ NMR and $^{13}C\{^{1}H\}$ NMR spectra were recorded on a Bruker DRX300 spectrometer operating at 300.13 MHz ($^{1}H$), 121.49 MHz ($^{31}P$), 282.40 MHz ($^{19}F$) and 75.47 MHz ($^{13}C$), respectively. Peak positions are relative to tetramethylsilane and were calibrated against the residual solvent resonance ($^{1}H$) or the deuterated solvent multiplet ($^{13}C$). Chemical shifts for $^{31}P\{^{1}H\}$ NMR were measured relative to external 85% $H_3PO_4$, and for $^{19}F\{^{1}H\}$ NMR to $CFCl_3$, they were measured with downfield values taken as positive in both cases. Infrared spectra were recorded on KBr discs using an FT-IR ATI Mattson Infinity Series. Elemental analysis (C, H, N, S) was performed on a Fisons Instruments EA1108 elemental analyser.

### 2.2. Synthesis of $[\{RuCp(mPTA)_2\}_2$-μ-(MBTT-k*S7,S´7*)$](CF_3SO_3)_4$ (1)

The bis-thiopurine $MBTTH_2$ (0.016 g, 0.036 mmol) was added into 10 mL of an aqueous solution of KOH (0.0075 M) and the initial mixture stirred until complete dissolution of the ligand. When dissolved the complex $[RuClCp(mPTA)_2](CF_3SO_3)_2$ (0.055 mg, 0.065 mmol) was added and refluxed for 4 h. The resulting mixture was cooled, filtered and concentrated by

evaporation to 1 mL. The obtained precipitate was filtered, washed with EtOH (2x 2 mL), $Et_2O$ (2 x 2 mL) and vacuum dried.

Yield powder: 0.057 g, 87%. $S_{25\,°C,H_2O}$(mg/mL): 30. Log *P*: -0.38. Elemental analysis for $C_{57}H_{84}N_{20}F_{12}O_{16}P_4Ru_2S_6$ (2051.81 g.mol$^{-1}$): Found C, 33.42; H, 4.18; N, 13.51; S, 9.23 %; calcd. C, 33.37; H, 4.13; N, 13.65; S, 9.38%. IR (KBr, cm$^{-1}$): $\nu$(C2=O) 1681 (s); $\nu$(C6=O) 1635 (s); $\nu$(C=C+C=N) 1523 (s); $\nu$(SO) 1226 (s). $^1$H RMN (20 ºC, $D_2O$): $\delta$ 2.78 (s, C**H**$_3$N$_{mPTA}$, 12H); 3.26 (s, C**H**$_3$N1$_{MBTT}$, 6H); 3.47 (s, C**H**$_3$N3$_{MBTT}$, 6H); 3.71-3.98 (m, NC**H**$_2$P$_{mPTA}$, 24H); 4.11-4.86 (m, NCH$_2$N$_{mPTA}$+ C**H**$_2$S$_{MBTT}$, 24H+2H); 5.02 (s, Cp, 10H). $^{13}$C{$^1$H} RMN (20 ºC, DMSO-$d_6$): $\delta$ 16.69 (s, CH$_2$S$_{MBTT}$); 28.12 (s, **C**H$_3$N1$_{MBTT}$); 30.64 (s, CH$_3$N3$_{MBTT}$); 49.21 (s, CH$_3$N$_{mPTA}$); 52.55 (d, $^1J_{CP}$ = 51.80 Hz, N**C**H$_2$P$_{mPTA}$); 60.57 (bd, $^1J_{CP}$ = 58.0 Hz, CH$_3$N**C**H$_2$P$_{mPTA}$); 68.68 (s, N**C**H$_2$N$_{mPTA}$); 79.84 (s, CH$_3$N**C**H$_2$N$_{mPTA}$); 84.23 (s, C$_p$); 114.63 (s, C5$_{MBTT}$); 119.53 (q, $^1J_{CP}$ = 316.86 Hz, $OSO_2CF_3$); 149.92 (s, C4$_{MBTT}$); 153.32 (s, C8$_{MBTT}$); 160.41 (s, C6$_{MBTT}$); 169.24 (s, C2$_{MBTT}$). $^{31}$P{$^1$H} RMN (20 ºC, $D_2O$): $\delta$ -7.85 (s, mPTA). $^{19}$F NMR ($D_2O$): $\delta$ -78.94 (s). Cyclic voltammetry (DMF, 22 °C): $E_{ox}$ = 0.706 V, 0.880 V.

### 2.3. Synthesis of [{RuCp(mPTA)$_2$}$_2$-μ-(EBTT-k*S7,S´7*)](CF$_3$SO$_3$)$_4$ (2)

Complex **2** was synthesized by a similar method than that described previously for **1**. The ligand $EBTTH_2$ (12.35 mg, 0.026 mmol) was dissolved into 10 mL of an aqueous solution of KOH (0.0053 M) before adding [RuClCp(mPTA)$_2$](CF$_3$SO$_3$)$_2$ (42.00 mg, 0.050 mmol). The final product is yellow.

Yield powder: 0.0325 g, 60%. $S_{25\,°C,H_2O}$(mg/mL): 12. Log *P*: -0.49. Elemental analysis for $C_{58}H_{86}F_{12}N_{20}O_{16}P_4Ru_2S_6$ (2056.84 g.mol$^{-1}$): Found C, 33.76; H, 4.28; N, 13.56; S, 9.22 %; calcd. C, 33.72; H, 4.20; N, 13.56; S, 9.31 %. IR (KBr, cm$^{-1}$): $\nu$(C2=O) 1683 (s); $\nu$(C6=O) 1630 (s); $\nu$(C=C+C=N) 1521 (s). $^1$H RMN (20 ºC, $D_2O$): $\delta$ 2.75 (s, C**H**$_3$N$_{mPTA}$, 12H); 3.34 (s, C**H**$_3$N1$_{EBTT}$, 6H); 3.86 (s, C**H**$_3$N3$_{EBTT}$, 6H); 3.81-4.93 (m, C**H**$_2$S$_{EBTT}$+NCH$_2$P$_{mPTA}$+ NCH$_2$N$_{mPTA}$, 4H+24H+24H); 4.87 (s, Cp, 10H). $^{13}$C{$^1$H} RMN (20 ºC, DMSO-$d_6$): $\delta$ 27.80 (s, **C**H$_3$N1$_{EBTT}$); 30.25 (s, **C**H$_3$N3$_{EBTT}$); 32.35 (s, **C**H$_2$S$_{EBTT}$); 48.58 (s, **C**H$_3$N$_{mPTA}$);

52.33 (d, $^{1}J_{CP}$ = 50.78 Hz, N**C**$H_2P_{mPTA}$); 61.14 (bd, $^{1}J_{CP}$ = 58.0 Hz, $CH_3N$**C**$H_2P_{mPTA}$); 68.77 (s, N**C**$H_2N_{mPTA}$); 78.10 (s, $CH_3N$**C**$H_2N_{mPTA}$); 82.51 (s, $C_p$); 116.80 (s, $C5_{EBTT}$); 118.87 (q, $^{1}J_{CP}$ = 316.85 Hz, $OSO_2CF_3$); 151.34 (s, $C4_{EBTT}$); 151.78 (s, $C8_{EBTT}$); 156.46 (s, $C6_{EBTT}$); 157.64 (s, $C2_{EBTT}$). $^{31}P\{^{1}H\}$ RMN (20 ºC, $D_2O$): $\delta$ -8.51 (s, mPTA). $^{19}F$ NMR ($D_2O$): $\delta$ -78.91 (s). Cyclic voltammetry (DMF, 22 °C): $E_{ox}$ = 0.546 V, 0.826 V.

### 2.4. Synthesis of [{RuCp(mPTA)$_2$}$_2$-μ-(PBTT-k*S7,S´7*)](CF$_3$SO$_3$)$_4$ (3)

Similarly to previous methods, the bis-thiopurine $PBTTH_2$ (0.014 g, 0.031 mmol) was dissolved in 10 mL of KOH in water (0.0067 M) and reacted with $[RuClCp(mPTA)_2](CF_3SO_3)_2$ (0.040 g, 0.054 mmol) at refluxing temperature to give finally a yellow powder.

Yield powder: 0.0325 g, 58%. $S_{25\,ºC,H_2O}$(mg/mL): 15.0. Log *P*: -0.55. Elemental analysis for $C_{59}H_{88}F_{12}N_{20}O_{16}P_4Ru_2S_6$ (2079.87 g.mol$^{-1}$): Found. C, 34.07; H, 4.34; N, 13.38; S, 9.13 %; calcd. C, 34.15; H, 4.26; N, 13.47; S, 9.25%. IR (KBr, cm$^{-1}$): ν(C2=O) 1682 (s); ν(C6=O) 1634 (s); ν(C=C+C=N) 1544 (s); ν(SO) 1224 (s). $^{1}H$ RMN (20 ºC, $D_2O$): $\delta$ 2.05 (q, $CH_2C$**H**$_2S_{PBTT}$, 2H), 2.77 (s, C**H**$_3N_{mPTA}$, 12H); 3.18 (s, C**H**$_3N1_{PBTT}$, 6H); 3.32 (s, C**H**$_3N3_{PBTT}$, 6H); 3.45 (t, C**H**$_2S_{PBTT}$), 4H); 3.84-4.10 (m, NC**H**$_2P_{mPTA}$, 24H); 4.30-4.57 (m, NC**H**$_2N_{mPTA}$, 24H); 4.88 (s, Cp, 10H). $^{13}C\{^{1}H\}$ RMN (20 ºC, DMSO-$d_6$):$\delta$ 28.08 (s, **C**$H_3N1_{PBTT}$); 29.73 (s, $CH_3N3_{PBTT}$); 30.05 (s, $CH_2$**C**$H_2S_{PBTT}$); 30.51 (s, **C**$H_2S_{PBTT}$); 48.60 (s, **C**$H_3N_{mPTA}$); 51.68 (d, $^{1}J_{CP}$= 50.80 Hz, N**C**$H_2P_{mPTA}$); 60.08 (bd, $^{1}J_{CP}$ = 58.15 Hz, $CH_3N$**C**$H_2P_{mPTA}$); 68,78 (s, N**C**$H_2N_{mPTA}$); 78.12 (s, $CH_3N$**C**$H_2N_{mPTA}$); 81.76 (s, $C_p$); 118.82 (q, $^{1}J_{CP}$ = 316.80 Hz, $OSO_2CF_3$); 116.64 (s, $C5_{PBTT}$); 151.24 (s, $C4_{PBTT}$); 153.64 (s, $C8_{PBTT}$); 158.75 (s, $C6_{PBTT}$); 166.00 (s, $C2_{PBTT}$). $^{31}P\{^{1}H\}$ RMN (20 ºC, $D_2O$): $\delta$ -8.52 (s, mPTA). $^{19}F$ NMR ($D_2O$): $\delta$ -78.95 (s). Cyclic voltammetry (DMF, 22 °C): $E_{ox}$ = 0.469 V, 0.813 V.

### 2.5. Stability tests of the complexes with $O_2$ and $H_2O$

The ruthenium complexes **1**, **2** and **3** were air stable for months in the solid state and for two days in solution. In a general procedure, the complex

(0.01 g) was introduced into a 5 mm NMR tube and dissolved in 0.5 mL of $D_2O$, the solution cooled at 4 ºC and then dry $O_2$ bubbled for 2 min via a long syringe needle. $^{31}P\{^1H\}$ NMR showed that no significant changes were produced in two days at room temperature. No significant decomposition was observed after one days at 40 °C as well. Sequential additions of 50 µL of DMSO-$d_6$ did not produce any significant change in the starting complexes after one days at 40 °C.

### 2.6. Cyclic voltammetry experiments

Electrochemical experiments were performed with a VersaSTAT3 apparatus. A standard disposition for the measurement cell was used including a three-electrode glass cell consisting of a platinum disk-working electrode, a platinum-wire auxiliary electrode and an Ag reference electrode. The supporting electrolyte solution ($LiClO_4$, 0.05 M) was scanned over the solvent window to verify the absence of electro-active impurities. A similar concentration of the analyte (0.1 mM) in $H_2O$ was employed in all the measurements.

### 2.7. Octanol-Water Partition Coefficient Determination

Accurate Log *P* values corresponding to the octanol-water partition coefficient [13] was adjusted to the solubility properties of the complexes. Complexes were dissolved in octanol previously saturated with distilled water with concentration range between $10^{-4}$ and $10^{-3}$ M. Into a 40 mL container at 25±1 ºC with a magnetic stir bar was introduced initially 10 mL of water previously saturated with octanol and then by a syringe 10 mL of the complex solutions in octanol, one so that the solution did not emulsify. Samples were taken from the octanol and water phases with a syringe until complex concentration in both phases stabilized, which was measured by UV-vis spectroscopy.

## 2.8. Growth Inhibition Assays

Cell growth inhibition assays were carried out using the *cis*platin-sensitive T2 human cell line and the *cis*platin-resistant SKOV3 cell line. T2 is a cell hybrid obtained by the fusion of the human lynphoblastoid line 174 (B lynphocyte transformed by the Epstein-Barr virus) with the CEM human cancer line (leukaemia T) while SKOV3 is derived from a human ovarian tumour. The cells were seeded in triplicate in 96-well trays at a density of $50 \cdot 10^3$ in 50 μl of AIM-V medium for T2, $25 \cdot 10^3$ in 50 μl of AIM-V medium for SKOV3. Stock solutions (10 mM) of the Ruthenium complexes **1-3** were made in DMSO and diluted in AIM-V medium to give final concentration of 2, 10 and 50 μM. *Cis*platin was employed as a control for the *cis*platin-sensitive T2 cell line and for the *cis*platin-resistant SKOV3. Untreated cells were placed in every plate as a negative control. The cells were exposed to the compounds for 72 h and then 25 μl of a 4,5-dimethylthiozol-2-yl)2,5-diphenyltetrazolium bromide solution (12 mM) were added. After two hours of incubation, 100 μl of lysing buffer (50% DMF + 20% SDS, pH 4.7) were added to convert 4,5-dimethylthiazol-2-yl-2,5-diphenyltetrazolium bromide into a brown coloured formazane. After additional 18 hours the solution absorbance, proportional to the number of live cells, was measured by spectrophotometer and converted in % of growth inhibition [14].

## 2.9. Calculation details

DFT calculations at B3LYP [15] level geometry optimizations of **1** - **3** in vacuum were carried out using NWCHEM 6.3 software package [16]. A Gaussian basis set of 3-21g was used for the structure optimization.

## 3. Results and discussion

### 3.1. Synthesis and characterization of 1–3

The dinuclear ruthenium complexes **1, 2** and **3** were obtained by reaction respectively of $MBTTH_2$, $EBTTH_2$ and $PBTTH_2$ with KOH and 2 equiv of $RuClCp(mPTA)_2](CF_3SO_3)_2$ in refluxing water (scheme 1).

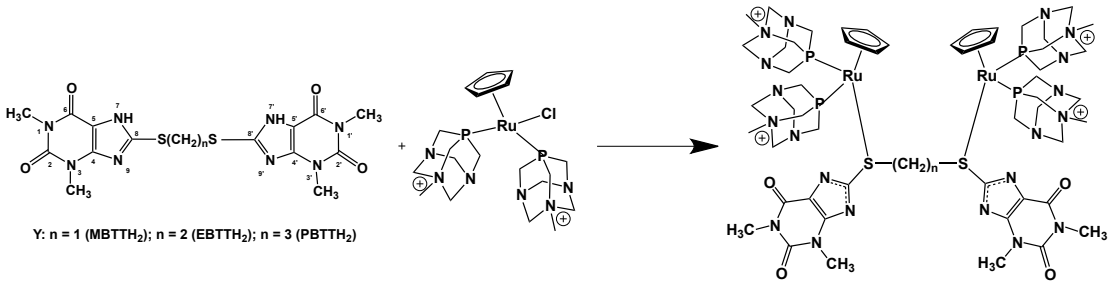


Scheme 1. Synthesis of **1**, **2**, and **3**.

The three complexes are yellow, soluble in water, DMSO and DMF but very low soluble in organic solvents. They are stable in solid state for months and in water for two days at room temperature and one day at 40 ºC also when DMSO-$d_6$ was added. The additional mPTA ligand provides to the new bi-metallic complexes **1**, **2** and **3** more water-solubility than those for the parent complexes [{RuCp($PPh_3$)(PTA)}$_2$-μ-(Y-κ*S7,S′7*)] [9], [{RuCp(PTA)$_2$}$_2$-μ-(Y-κ*S7,S′7*)] [9] and [{RuCp($PPh_3$)(mPTA)}$_2$-μ-(L-κ*S7,S′7*)] [10]. The elemental analyses of the complexes were in agreement with a proportion of two $\{CpRu(mPTA)_2\}^{2+}$ units to one bis-thiopurine molecule. The $^{31}P\{^1H\}$ NMR spectra for the three complexes show a singlet at -7.85 ppm (**1**), -8.51 ppm (**2**), and -8.52 (**3**). The $^1H$ NMR ($D_2O$) signals only could be assigned using $^1H,^1H$-2D COSY NMR, and by comparison with those for the parent previously published bimetallic Ru complexes: [{RuCp($PPh_3$)(PTA)}$_2$-μ-(L-κ*S7,S′7*)] [9] and [{RuCp(PTA)$_2$}$_2$-μ-(L-κ*S7,S′7*)] [9] and [{RuCp($PPh_3$)(mPTA)}$_2$-μ-(L-κ*S7,S′7*)] [10]. The resonances for N1$CH_3$ and N3$CH_3$ were observed indicating the presence of the purines [9,10]. The **1** S–$CH_2$–S broad signal (4.50 ppm) is in the range found for the mPTA-$CH_2$ signals, which is similar to

those found for [{RuCp(PPh$_3$)(PTA)}$_2$-μ-(L-κ*S7,S′7*)] (4.62 ppm) [9], [{RuCp(PPh$_3$)(mPTA)}$_2$-μ-(L-κ*S7,S′7*)] (4.68 ppm) [10] *cis*-[{PtCl(PPh$_3$)$_2$}$_2$(μ-MBTT-κ*N7,N7′*)] (5.0 ppm) [22], *cis*-[{Pt(PTA)$_2$}$_2$(μ-Cl)(μ-MBTT-κ*N7,N7′*)]Cl (4.21 ppm) [12a] and *trans*-[{PdCl(PPh$_3$)$_2$}$_2$(μ-MBTT-κ*N7,N7′*)] (4.15 ppm) [12b].

In the $^1$H NMR of **2** the four S(CH$_2$)$_2$S protons are chemically different and arise as multiplets in similar range that those found from 3.81 to 4.93 ppm that is somewhat shifted to low field than those found in similar ruthenium complexes containing this ligand, Cp, and PTA: [{RuCp(PPh$_3$)(PTA)}$_2$-μ-(L-κ*S7,S′7*)] (2.72 ppm to 3.62 ppm) [9], [{RuCp(PTA)$_2$}$_2$-μ-(L-κ*S7,S′7*)] (3.17 to 3.44 ppm) [9] and [{RuCp(PPh$_3$)(mPTA)}$_2$-μ-(L-κ*S7,S′7*)] (2.86 to 3.10 ppm) [10]. In the few known EBTT$^{2-}$ complexes with other metals a broad singlet was observed for this group: *trans*-[{PdCl(PPh$_3$)$_2$}$_2$(μ-EBTT-κ*N7,N′7*)] (S-(CH$_2$)$_2$-S = 2.87 ppm) [13c] and *cis*-[{Pt(PTA)$_2$}$_2$(μ-Cl)(μ-EBTT-κ*N7,N7′*)]Cl (S-(CH$_2$)$_2$-S = 1.92 ppm) [13c]. This fact suggests that the ligand EBTT$^-$ coordinates more through the closer sulfur, which are bonded to the –CH$_2$–CH$_2$– group, than through the two distant imidazolic N7 atoms.

The $^1$H NRM spectrum of **3** displays the Cp as a broad signal and the S-(CH$_2$)$_3$-S signals as multiplets at chemical shifts (-CH$_2$- = 2.05 ppm; S-CH$_2$- = 3.45 ppm) rather different to those for free PBTTH$_2$ (-CH$_2$- = 2.17 ppm; S-CH$_2$- = 3.40 ppm) and coordinated PBTT$^{2-}$ in complexes: [{RuCp(PPh$_3$)(PTA)}$_2$-μ-(L-κ*S7,S′7*)] (-CH$_2$- = 2.20 ppm; S-CH$_2$- = 3.22, 4.48 ppm) [9], [{RuCp(PTA)$_2$}$_2$-μ-(L-κ*S7,S′7*)] (-CH$_2$- = 1.56 ppm; S-CH$_2$- = 2.95, 4.46 ppm) [9], [{RuCp(PPh$_3$)(mPTA)}$_2$-μ-(L-κ*S7,S′7*)] (-CH$_2$- = 2.08 ppm; S-CH$_2$- = 3.37 ppm) [10], *cis*-[{Pt(PTA)$_2$}$_2$(μ-Cl)(μ-PBTT-κN7,N′7)]Cl (-CH$_2$- = 2.03 ppm; S-CH$_2$- = 3.39 ppm) [13] and *trans*-[{PdCl(PPh$_3$)$_2$}$_2$(μ-PBTT-κ*N7,N′7*)] (-CH$_2$- = 2.56 ppm; S-CH$_2$- = 3.72 ppm) [13c]. This result supports newly that sulfurs are the probable coordination point of PBTT$^-$ in **3**.

The $^{13}$C{$^1$H} NMR spectrum of **1** shows the SCH$_2$S and C8 signals (S-CH$_2$-S = 36.21 ppm; C8 = 153.32 ppm) with a chemical shift very close to those found for *cis*-[{Pt(PTA)$_2$}$_2$(μ-Cl)(μ-MBTT-κN7,N7′)]Cl (S-CH$_2$-S = 35.85 ppm; C8 = 150.52 ppm) [7b] and *trans*-[{PdCl(PPh$_3$)$_2$}$_2$(μ-MBTT-κ*N7,N7′*)] (S-CH$_2$-S = 36.90 ppm; C8 = 150.30 ppm) [13c] and published MBTT-Cp-PTA

ruthenium complexes [{RuCp($PPh_3$)(PTA)}$_2$-μ-(MBTT-κ*S7,S′7*)] (S-$CH_2$-S = 33.95 ppm; C8 = 151.85 ppm) [9], [{RuCp(PTA)$_2$}$_2$-μ-(MBTT-κ*S7,S′7*)] (S-$CH_2$-S = 38.07 ppm; C8 = 153.83 ppm) [9] and [{RuCp($PPh_3$)(mPTA)}$_2$-μ-(MBTT-κ*S7,S′7*)] (S-$CH_2$-S = 35.53 ppm; C8 = 151.12 ppm) [10]. While in **2** the S$(CH_2)_2$S and C8 signals (S-$(CH_2)_2$-S = 32.35 ppm; C8 = 151.78 ppm) are similar to those for free EBTT$H_2$ (S-$(CH_2)_2$-S = 32.00 ppm; C8 = 148.10 ppm) and the reported complexes [{RuCp($PPh_3$)(PTA)}$_2$-μ-(EBTT-κ*S7,S′7*)] (S-$(CH_2)_2$-S = 32.38 ppm; C8 = 150.6 ppm) [9], [{RuCp(PTA)$_2$}$_2$-μ-(EBTT-κ*S7,S′7*)] (S-$(CH_2)_2$-S = 34.74 ppm; C8 = 151.68 ppm) [9], [{RuCp($PPh_3$)(mPTA)}$_2$-μ-(EBTT-κ*S7,S′7*)] (S-$CH_2)_2$-S = 32.21 ppm; C8 = 151.67 ppm) [10]., *cis*-[{Pt(PTA)$_2$}$_2$(μ-Cl)(μ-N,N-EBTT)]Cl (S-$(CH_2)_2$-S = 35.85 ppm; C8 = 150.52 ppm) [7b] and *trans*-[{PdCl($PPh_3$)$_2$}$_2$(μ-EBTT-κ*N7,N′7*)] (S-$(CH_2)_2$-S = 32.70 ppm; C8 = 150.90 ppm) [13c]. Complex **3** displays a similar $^{13}C\{^1H\}$ NMR spectrum to those ruthenium complexes with PBTT and mPTA ligands previously published. The chemical shifts of the bridging $CH_2$ and C8 carbons in **3** (-$CH_2$- = 30.05 ppm; C8 = 153.64 ppm) are similar to those for [{RuCp(PTA)$_2$}$_2$-μ-(PBTT-κ*S7,S′7*)] (-$CH_2$- = 28.30 ppm; S-$CH_2$- = 30.51 ppm; C8 = 149.73 ppm) [{RuCp($PPh_3$)(PTA)}$_2$-μ-(PBTT-κ*S7,S′7*)] (-$CH_2$- = 30.23 ppm; C8 = 152.06 ppm) [9], [{RuCp(PTA)$_2$}$_2$-μ-(PBTT-κ*S7,S′7*)] (-$CH_2$- = 28.30 pp; C8 = 149.73 ppm) [9] and [{RuCp($PPh_3$)(mPTA)}$_2$-μ-(PBTT-κ*S7,S′7* (-$CH_2$- = 29.73 ppm; S-$CH_2$- = 30.52 ppm; C8 = 148.91 ppm) [10]., but those signals for S$CH_2$ in the complexes [{RuCp($PPh_3$)(PTA)}$_2$-μ-(PBTT-κ*S7,S′7*)] (44.11 ppm) [9] and [{RuCp(PTA)$_2$}$_2$-μ-(PBTT-κ*S7,S′7*)] (45.87 ppm) [9] display quite different chemical shifts than S-$CH_2$- of **3** (30.51 ppm). Nevertheless, the propyl protons display a comparable chemical shift to those in **3**, PBTT$H_2$ (-$CH_2$- = 29.20 ppm; S-$CH_2$- = 30.20 ppm; C8 = 148.20 ppm) and in the reported complexes *cis*-[{Pt(PTA)$_2$}$_2$(μ-Cl)(μ-PBTT-κ*N7,N′7*)]Cl (-$CH_2$- = 32.00 ppm; S-$CH_2$- = 32.20 ppm; C8 = 151.86 ppm) [7b] and *trans*-[{PdCl($PPh_3$)$_2$}$_2$(μ-PBTT-k*N7,N′7*)] (-$CH_2$- = 28.60 ppm; S-$CH_2$- = 30.40 ppm; C8 = 151.00 ppm) [13c]. The solubility of three complexes in available solvents were not enough for a clear observation of $CF_3SO_3^-$ signals. The presence in solution of non-coordinated triflate anions was supported by the presence of a unique singlet at ca. -78.90 ppm in their $^{19}F$ NMR.

Unfortunately it was not possible to obtain crystals good enough for determining the crystal structure of these complexes by single X-ray diffraction after numerous attempts. However, the spectroscopic evidence supports that the most probable structures for **1**, **2** and **3** are those displayed in Scheme 1, where each S of the bis-thiotheophylline derivative is bonded to a Ru, which completes its coordination geometry with an $\eta^5$-Cp and two mPTA bonded by the P atom. The three complexes were studied by $^1$H DOSY experiments in order to obtain the diffusion diameter of the molecules in water that could support the bimetallic nature of them. The obtained value for the diffusion constant of **1** ($2.62 \cdot E^{-10}$ $m^2/s$, SI) corresponds to a hydrodynamic radius of 9.36 Å [17], which is somewhat bigger than that found for the parent bimetallic ruthenium complex $[(PTA)_2CpRu\text{-}\mu\text{-}CN\text{–}RuCp(PTA)_2]^+$ (9.09 Å) [18]. Unfortunately the $^1$H DOSY experiments for complexes **2** and **3** did not provided information reliable of the hydrodynamic radius of these complexes, which could be produced for a large hydrogen network in solution as indicated previously for ruthenium complexes containing PTA derivatives [19].

The energy of the proposed composition of the complexes was calculated by theoretical procedures to obtain a final support for their composition. Initially the similar neutral bis-ruthenium molecules containing PTA were calculated (Supporting Information) by using previously obtained single-crystal X-ray structures [20]. The coordinates and energy for the calculated structures were included in the Supporting Information.

The optimized molecular geometries of complexes **1**, **2** and **3** are shown in Figure 1 and their cartesian coordinates display in Supporting Information. The theoretical study showed that in gas phase the κ*S*-complexes containing PTA and mPTA display similar stability, being those of mPTA somewhat larger than those with PTA (S14, SI). and those found in parent calculated complexes [21]. The calculated structures for **1**, **2** and **3** κ*S*-complexes are in agreement with the X-ray structures of $[RuCp(8MTT\text{-}\kappa S)(mPTA)_2]Cl(CF_3SO_3)$ [21] although optimized Ru-P and Ru-S bond lengths are larger than crystalline ones. Similar deviations were found in bibliography for Ru(II)-complex structures when calculated at B3LYP/DZVP and B3LYP/LANL2DZ levels [22].

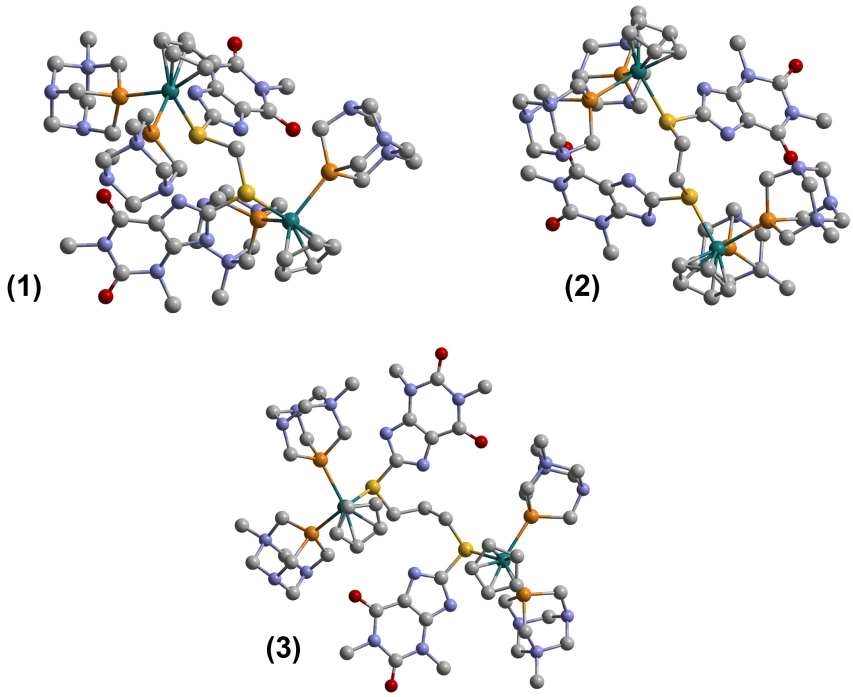


Figure 1. B3LYP/3-21G optimized structures of **1**, **2** and **3**. For the sake of clarity hydrogens are not shown.

Selected bond lengths and angles for optimized structures of complexes **1**, **2** and **3** are shown in Table 1. The three complexes show a similar piano stool structure in which the purines are basically planar. It is interesting to stress that the disposition of the purine with respect to the Cp changes significantly from **1** (purine-plane-A/Cp1-plane = 19.32º; purine-plane-B/Cp1-plane = 71.52º; purine-plane-A/Cp2-plane = 78.36º; purine-plane-B/Cp2-plane = 38.44º) to **2** (purine-plane-A/Cp1-plane = 23.61º; purine-plane-B/Cp1-plane = 62.23º; purine-plane-A/Cp2-plane = 74.59º; purine-plane-B/Cp2-plane = 11.08º) and **3** (purine-plane-A/Cp1-plane = 53.76; purine-plane-B/Cp1-plane = 17.52º; purine-plane-A/Cp2-plane = 78.36º; purine-plane-B/Cp2-plane = 29.22º). The purine-A and purine-B being that coordinated respectively to Ru1 and Ru2.

**Table 1**. Selected Bond Distances (Á) and Angles (deg) for calculated structures for **1** (A), **2** (B) and **3** (C).

| | **1** | **2** | **3** |
|---|---|---|---|
| Ru1 – P1 | 2.582 | 2.590 | 2.54 |
| Ru1 – P2 | 2.557 | 2.580 | 2.556 |
| Ru1 – S | 2.544 | 2.524 | 2.544 |
| Ru1-$Cp_{(centroid)}$ | 1.698 | 1.697 | 1.700 |
| C8t – N7t | 1.334 | 1.334 | 1.334 |
| C5t – N7t | 1.395 | 1.394 | 1.395 |
| P1 – Ru1 – P2 | 96.47 | 96.88 | 101.81 |
| P1 – Ru1 – S | 86.87 | 84.77 | 88.70 |
| P2 – Ru1 – S | 92.72 | 92.36 | 92.03 |
| C8t – S – Ru1 | 109.47 | 109.77 | 109.44 |
| C5t – S – Ru1 | 119.19 | 119.77 | 110.26 |

The HOMO orbitals of the complexes (The orbital energies and composition in terms of fragments contributions for the most significant frontier molecular orbitals are shown in S37, SI) are mainly constituted by the 8-MBTT-HOMO-orbitals that slightly overlaps through one of the S lobes (**1**: 4 %; **2**: 5 %; **3**: 6 % contribution) with one of the Ru-d orbitals (**1**: 2 %; **2**: 3 %; **3**: 4 % contribution). The LUMO orbitals of **2** and **3** are similar but quite different from **1**, being the main contribution to the LUMO of **2** and **3** the Ru2 (**2**: 46 %; **3**: 48 %) orbital and in minor grade the purine, Cp2, mPTA3 and mPTA4 orbitals. In contrast the main contributions in **1** are both metals (Ru1: 19 %; Ru2: 31 %) and there are contributions of all the other molecule groups, being the minor that for the phospines (mPTA1:2 %; mPTA2 = 3 %; mPTA3 = 3 %; mPTA4 = 3 %). Therefore, the complexes **1**, **2** and **3** are similarly stable to the

known ruthenium complexes containing mPTA and thiopurines, which also justified the preferred coordination through S is drawn from them.

### 3.2. Electrochemistry of 1–3

The redox properties of **1**, **2** and **3** in $H_2O$ were studied to obtain information on the redox behavior of two ruthenium metals bonded to close purines in comparison with the previously published bis-ruthenium-8-bis-thiotheophyllyne complexes. The three complexes exhibited an irreversible redox behavior (Figure 2). All the recorded electrode potentials were in a short range similar to those found for ruthenium complexes containing Cp and PTA [23]. The three oxidation waves for the complexes only can be assigned to single-electron charge transfer of two independent Ru centers ($Ru^{II}Ru^{II}/Ru^{III}Ru^{II}$ and $Ru^{III}Ru^{II}/Ru^{III}Ru^{III}$) and therefore, support the proposed bimetallic character for the complexes [10,24,25]. It is interesting to stress that also for these complexes the oxidation potentials decrease linearly when the bispurine-alkyl-bridging group increases in length ($E_{ox}(1)$ = 706 mV (**1**); 546 mV (**2**); 469 mV (**3**); $E_{ox}(2)$ = 880 mV (**1**); 826 mV (**2**); 813 mV (**3**)). The alkyl size and, therefore, the link size between purines have a clear influence on the redox properties of the $\{CpRu(mPTA)_2\}^{2+}$ moiety (Figure 3). There are no electronic connections between both metals through the alkyl bridging group and through the solvent is also improbable, but clearly there is a net influence of the bringing group size between the purines as observed previously in parent complexes [$\{RuCp(PPh_3)(PTA)\}_2$-μ-(PBTT-κ*S7,S′7*)], [$\{RuCp(PTA)_2\}_2$-μ-(PBTT-κ*S7,S′7*)] [9] and [$\{RuCp(PPh_3)(mPTA)\}_2$-μ-(L-κ*S7,S′7*)] [10]. The calculated energy difference ∆(HOMO-LUMO) is in agreement with that tendency as it is 3532 eV for **1**, 3345 eV for **2** and 3584 eV for **3**. Thus, the correlation between the observed redox potentials and the alkyl linking group size is correlated with the energy of the orbitals and with the redox properties of the complexes. Nevertheless deeper studies and more precise calculations should be preformed before to consider that this is a general property of this kind of bis-ruthenium-8-bis-thiotheophylline complexes.

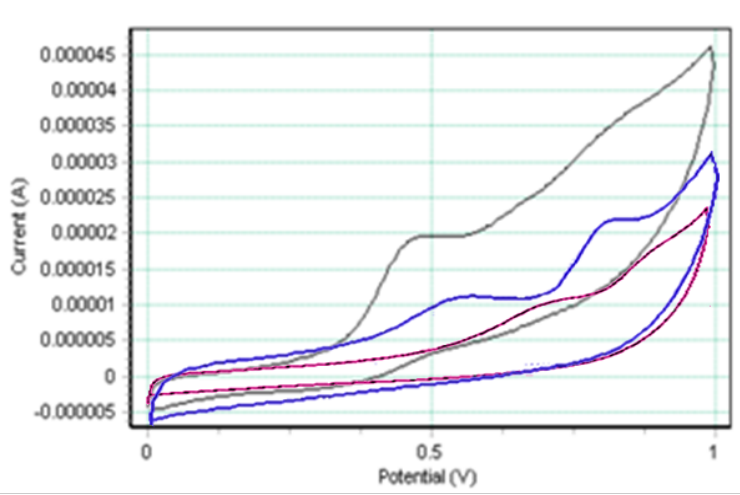


Figure 2. Cyclic voltammograms in $H_2O$ of **1** (red line), **2** (blue line) and **3** (black line)

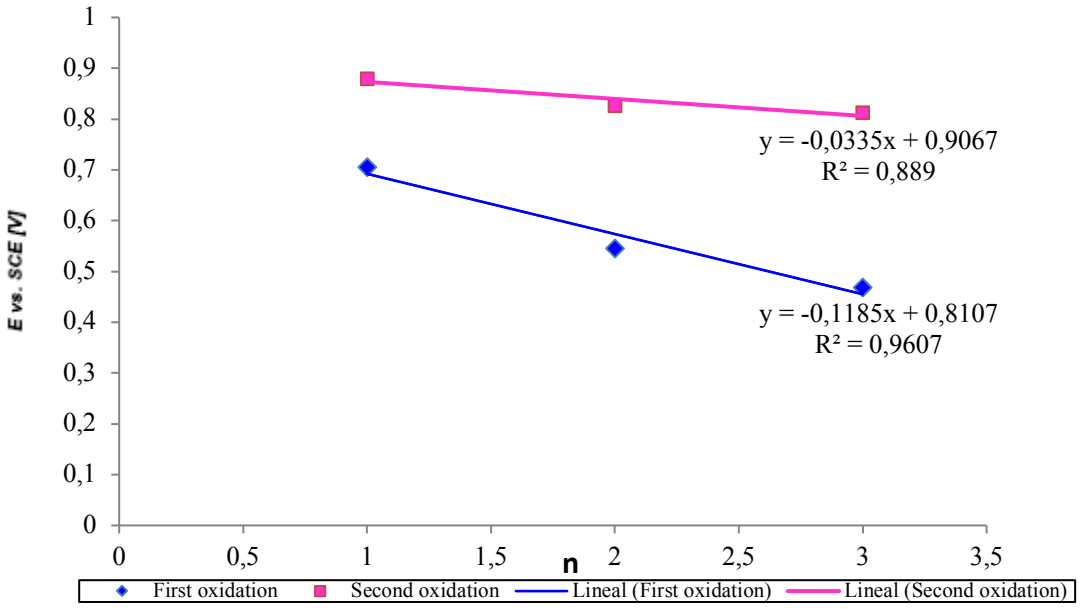


Figure 3. First and second oxidation potential *vs*. the numbers of alkyl group atoms for **1**, **2** and **3**.

**Cell Growth Inhibition.**

The complexes **1**-**3** have been tested for cell growth inhibition activity on the human cancer cell lines *cis*platin-sensitive T2 and the *cis*platin-resistant SKOV3 (results reported in Table 2). The growth inhibition activity values for *cis*platin and the precursors [RuClCp($PPh_3$)(PTA)] and [RuClCp$(PTA)_2$] were also obtained. Each complex was dissolved in DMSO

and diluted in AIM-V medium to obtain the final concentrations of 50, 10, and 2 μM solutions. The percentage of growth inhibition at the three doses for each complex allowed us to estimate the IC50, the concentration reducing to 50% the cell growth of both cell lines. Tests with the *cis*platin-sensitive cells T2 show that three complexes display a low activity as the precursor [RuClCp(PTA)$_2$]). Tests with the *cis*platin-resistant SKOV3 cell line showed that this complex are similarly active than *cis*platin on Pt-resistant cell line. This behaviour was previously related to the difficulty for hydrophilic mPTA complexes in crossing the lipophilic membranes of the cell and of the nucleus to reach the nucleic acids. This suspicion is in agreement with the determined partition coefficient Log *P* for each new complex (Table 2). Those complexes (**1**-**3**) with negative Log *P* as found for previously published parent complexes [9] do not display significant antiproliferative activity. Therefore, additionally to a favourable Log *P* also should be important to take in account the water solubility and the oxidation potential of the complexes. It was evidenced the redox capacities of the ruthenium complexes with their redox properties [9], the largest is the oxidation potential the higher the anticancer activity. The effect of the water solubility is also important but there was not until know any study that shows the exclusive effect of the water solubility with the antiproliferative activity.

**Table 2**. Estimated IC50 on *cis*platin sensitive T2 cell line and *cis*platin-resistant SKOV3 of complexes **1**-**3**, Log *P*, $S_{25,H_2O}$(mg/cm$^3$) and $E_o$.

| Complex | T2 | SKOV3 | Log *P* | $S_{25,H_2O}$(mg/cm$^3$) | $E_o$ (mV) |
|---|---|---|---|---|---|
| **1** | >50 μM | > 50 μM | -0.38 | 30.0 | 706, 880 |
| **2** | > 50 μM | > 50 μM | -0.49 | 12.0 | 546, 826 |
| **3** | >50 μM | > 50 μM | -0.45 | 15.0 | 469, 813 |
| *cis*-Pt | 2-10 μM | > 50 μM | | | |

## 4. Conclusion

The present work details the synthesis of $\eta^5$-Cp-ruthenium(II) complexes bearing the bis(S-8-thiotheophyllinate)methane ($MBTTH_2$), 1,2-bis(S-8-thiotheophyllinate)ethane ($EBTTH_2$) and 1,3-bis(S-8-thiotheophyllinate)propane alkane ($PBTTH_2$) and two ligands mPTA. These complexes display larger water solubility than those parent bis-thio-theophylline complexes [{RuCpLL'}$_2$-μ-(Y-κ*S7,S'7*)] (L, L' = PTA; L = $PPh_3$, L' = PTA, mPTA). The three complexes show two successive one-electron oxidations ($Ru^{II}Ru^{II}/Ru^{III}Ru^{II}$ and $Ru^{III}Ru^{II}/Ru^{III}Ru^{III}$) in agreement with the presence of two metals in the molecule. The redox potentials of the complexes decrease linearly increasing the bridging alkyl size of the bis(8-thiotheophylline) ligands that is also the same tendency observed for the HOMO-LUMO energy gap, which is probably correlated with the steric interaction among the different molecule group. A large theoretical and experimental study is needed to finally support that this a general property for this kind of complexes. The antiproliferative activities of complexes **1**, **2** and **3** against *cis*platin-sensitive T2 and the *cis*platin-resistant SKOV3 cancer cells were found to be non-relevant in comparison with those for parent mononuclear ruthenium complexes, probably due to the reduce solubility of this complexes in organic environments as showed by their partition coefficient.

## 5. Acknowledgements.

Thanks are given to the European Commission FEDER program for co-financing the projects CTQ2015-67384-R (MINECO) and P09-FQM-5402 (Junta de Andalucía). Thanks are also given to Junta de Andalucía PAI-research group FQM-317 and COST Action CM1302 (WG1, WG2). F. S. Thanks to University of Almeria for a predoctoral grant.

## References


[1] B. Rosenberg, L. Van Camp, T. Krigas. *Nature*, **205**, 698–699 (1965).

[2] V. Cepeda, M. A. Fuertes, J. Castilla, C. Alonso, C. Quevedo, J. M. Perez. *Anti-Cancer Agents Med. Chem*., **7**, 3 (2007).

[3] G. Giaccone, R. S. Herbst, C. Manegold, G. Scagliotti, R. Rosell, V. Miller. *J. Clin. Oncol*., **22**, 777 (2004).

[4] (a) G. Gasser, I. Ott, N. Metzler-Nolte. *J. Med. Chem*., **54**, 3 (2011); (b) M. A. Jakupec, M. Galanski, V.B. Arion, C.G. Hartinger, B.K. Keppler. *Dalton Trans.*, **2**, 183 (2008); (c) P. J. Dyson, G. Sava. *Dalton Trans.*, 1929, and references therein (2006).

[5] (a) M. Clarke. *J. Coord. Chem. Rev.*, **236**, 209 (2003); (b) G. S. Smitha, B. Therrien. *Dalton Trans.*, **40**, 10793 (2011). (b) Q. Wu, K. Zheng, S. Liao, Y. Ding, Y. Li, W. Mei. *Organometallics* **35**, 317−326 (2016); (b) Q. Wu, T. Chen, Z. Zhang, S. Liao, X. Wu, J. Wu. *Dalton Trans.* **43**, 9216-9225 (2014); (c) Q. Wu, J. He, W. Mei, Z. Zhang, X. Wuc, F. Sun. *Metallomics* **6**, 2204-2212 (2014); (d) F. Hayat, Z-U. Rehman, M.H. Khan. *Journal of Coordination Chemistry* **70**, 279-295 (2017); (e) J.-Q. Wang, Z.-Z. Zhao, H.-B. Bo, Q.-Z. Chen. *Journal of Coordination Chemistry* **69**, 177-189 (2016); (f) J.M. Gichumbi, H.B. Friedrich, B. Omondi, M. Singh, K. Naicker, H.Y. Chenia. *Journal of Coordination Chemistry* **69**, 3531-3544 (2016). (g) C. Wang, Q. Wu, Y. Zeng, D. Huang, C. Yu, X. Wang, W. Mei. *Journal of Coordination Chemistry* **68**, 1489-1499 (2015).

[6] (a) I. Bratsos, S. Jedner, T. Gianferrara, *E.* Alessio. *Chimia*, **61**, 692 (2007); (b) F. Lentz, A. Drescher, A. Lindauer, M. Henke, R.A. Hilger, C. G. Hartinger, M.E. Scheulen, C. Dittrich, B. K. Keppler, U. Jaehde. *Anti-Cancer Drugs*, **20**, 97 (2009); (c) T. Gianferrara, I. Bratsos, E. Alessio. *Dalton Trans*., 7588 (2009).

[7] (a) Z. Mendoza, P. Lorenzo-Luis, M. Serrano-Ruiz, E. Martín-Batista, J. M. Padrón, F. Scalambra, A. Romerosa. *Inorg. Chem.*, **55**, 7820-7822 (2016); (b) A. Romerosa, P. Bergamini, V. Bertolasi, A. Canella, M. Cattabriga, R. Gavioli, S. Mañas, N. Mantovani, L. Pellacani. *Inorg. Chem*., **43**, 905 (2004); (c) P. Bergamini, V. Bertolasi, L. Marvellli, A. Canella, R. Gavioli, N.

Mantovani, S. Mañas, A. Romerosa. *Inorg.Chem*., **46**, 4267 (2007); (d) A. Romerosa, T. Campos-Malpartida, C. Lidrissi, M. Saoud, M. Serrano-Ruiz, M. Peruzzini, J.A. Garrido-Cardenas, F. Garcia-Maroto. *Inorg. Chem*., **45**, 1289 (2006).

[8] (a) A. Romerosa, T. Campos-Malpartida, C. Lidrissi, M. Saoud, M. Serrano-Ruiz, M. Peruzzini, J.A. Garrido-Cardenas, F. Garcia-Maroto. *Inorg. Chem*., **45**, 1289 (2006); (b) A. Mena-Cruz, P. Lorenzo-Luis, A. Romerosa, M. Saoud, M. Serrano-Ruiz. *Inorg. Chem.*, **46**, 6120 (2007); (c) A. Mena-Cruz, P. Lorenzo-Luis, A. Romerosa, M. Serrano-Ruiz. *Inorg. Chem*., **47**, 2246 (2008); (d) A. Mena-Cruz, P. Lorenzo-Luis, V. Passarelli, A. Romerosa, M. Serrano-Ruiz. *Dalton Trans*., 3237 (2011); (e) M. Serrano-Ruiz, L.M. Aguilera-Sáez, P. Lorenzo-Luis, J.N. Padrón, A. Romerosa. *Dalton Trans*.,11212 (2013).

[9] L. Hajji, C. Saraiba-Bello, A. Romerosa, G. Segovia-Torrente, M.Serrano-Ruiz, P. Bergamini, A. Canella. *Inorg. Chem*., **50**, 873 (2011).

[10] L. Hajji, S.B. Cristobal, A. Romerosa, S.T. Gaspar, S.R. Manuel. *J. Coordination Chemistry*, **67**, 16 (2014).

[ 11 ] D.D. Perrin, W.L.F. Armarego (Eds.). Purification of Laboratory Chemicals, 3rd ed., Butterworths and Heinemann, Oxford (1988).

[12] (a) A. Romerosa, C. López-Magaña, M. Saoud, S. Mañas. *Eur. J. Inorg. Chem.*, 348-355 (2003); (b) A. Romerosa, C. López-Magaña, A.E. Goeta, S. Mañas, M. Saoud, F.B. abdelouahab, F. El Guemmout. *Inorg. Chim. Acta*, **353**, 99-106 (2003); (c) *Aqueous-Phase Organometallic Catalysis*; Cornils B., Herrmann W. A., Eds.; Wiley-VCH, Weinheim, Germany (1998); (d) F. Joo, J. Kovacs, A. Katho, A. C. Benyei, T. Decuir, D. *J.* Darensboug. *Inorg. Synth*., **32**, 2 (1998); (e) A. Romerosa, C. López-Magaña, M. Saoud, E. Colacio, J. Suarez-Varela, *Inorg. Chim. Acta*, **307**, 125-130 (2000); (f) A. Romerosa, C. López-Magaña, S. Mañas, M. Saoud, A.E. Goeta. *Inorg. Chim. Acta*, **353**, 145-150 (2003).

[13] (a) R. Mannhold, G. I. Poda, C. Ostermann, I.G. Tetko. *J. Pharm. Sci.* **98**, 861-893 (2009); (b) H. R. Lozano, F. Martínez. *Braz. J. Pharm. Sci.* **42**, 601-613 (2006); (c) L. Ropel, L.S. Belvèze, S.N.V.K. Aki, M.A. Stadtherr, J.F. Brennecke. *Green. Chem.* **7**, 83–90 (2005).

[14] M.B. Hansen, S.E. Nielsen, K. J. Berg. *Immunol. Methods* **119**, 203 (1989).

[15] M.G. Sauaia, E. Tfouni, R.H. de Almeida Santos, M.T. do Prado Gambardella, M.P.F.M. Del Lama, L.F. Guimarães, R. Santana da Silva. *Inorg. Chem. Comm.* **7**, 864-867 (2003); (b) A. Szabo, N.S. Ostlund. *Modern Quantum Chemistry*, Dover Publications Inc., Mineola, New York, (1996); (c) A.D. Becke. *J. Chem. Phys.* **98**, 1372-1377 (1993); (d) C. Lee, W. Yang, R.G. Parr. *Phys. Rev. B* **37**, 785-789 (1988).

[16] M. Valiev, E. J. Bylaska, N. Govind, K. Kowalski, T.P. Straatsma, H.J.J. Van Dam, D. Wang, J. Nieplocha, E. Apra, T. L. Windus, W. A. de Jong. *Comput. Phys. Comm.* **181**, 1477-1489 (2010).

[17] (a) A. Macchioni, G. Ciancaleoni, C. Zuccaccia, D. Zuccaccia. *Chem. Soc. Rev.*, **37**, 479 (2008); (b) $D=(k_BT)/(6\pi\eta r_H)$, in which D is the diffusion coefficient, $k_B$ is the Boltzman constant, T is the temperature, and η is the viscosity of the solvent.

[18] F. Scalambra, M. Serrano-Ruiz, A. Romerosa. *Macromol. Rapid Commun.* **36**, 689-693 (2015).

[19] A. Mena-Cruz, Pablo Lorenzo-Luis, Vincenzo Passarelli, Antonio Romerosa, Manuel Serrano-Ruiz. Dalton Trans., **40**, 3237-3244 (2011)

[20] Cambridge Crystallographic Data Centre (CCDC), (2016).

[21] L. Hajji, V. Jara-Pérez, C. Saraiba-Bello, G. Segovia-Torrente, M. Serrano-Ruiz, A. Romerosa. *Inorganica Chimica Acta*, **455**, 557-567 (2017).

[22] B.D. Alexander, T.J. Dines, R.W. Longhurst, Chem. Phys. 352 (2008) 19.

[23] V. Gutkin, J. Gun, P.V. Prikhodchenko, O. Lev, L. Gonsalvi, M. Peruzzini, A. Romerosa, T. Malpartida, C. Lidrissi. *J. Electrochem. Soc.*, **154**, F7 (2007).

[24] M. Auzias, B. Therrien, G. Süss-Fink, P. Štěpnička, W.H. Ang, P.J. Dyson *Inorg. Chem*., **47**, 578 (2008).

[25] M. Gras, B. Therrien, G. Süss-Fink, P. Štěpnička, A.K. Renfrew, P.J. Dyson. *J. Organomet. Chem.*, **693**, 3419 (2008).